EFFECT OF DETECTOR AND ELECTRONICS FAULT ON PET RECONSTRUCTED IMAGE ACQUIRED WITH THE FULL RING HR+

E. Fusilli**, F. Zito*, E. De Bernardi**, M. Schiavini*, C. Canzi*,
F. Voltini*, S. Agosteo*** and P. Gerundini*

* Nuclear Medicine Department, Ospedale Maggiore Policlinico,
Mangiagalli e Regina Elena, Milan, Italy
** Biomedical Engineering Department, Polytechnic University of Milan, Italy
*** Nuclear Engineering Department, Polytechnic University of Milan, Italy

E-Mail zitom@policlinico.mi.it

Abstract: The influence of defective detector blocks on accuracy of PET reconstructed images was assessed qualitatively and quantitatively by using the ECAT HR+ scanner. A procedure to simulate defective block was carried out after analysing and comparing Blank scans obtained with detection system in good operation with those having some faulty block detectors. Different levels of detector damages were simulated and tested with phantom studies. The obtained results allowed to better know type and entity of artefact expected on reconstructed data and then to identify cases of malfunctioning blocks that really need to stop clinical activity.

Introduction

Calibration check and quality control of a PET scanner are routinely performed to guarantee the best detector performance and diagnostic accuracy. The status of the PET HR+ system is daily checked by using the Blank scan data. A report flagging the blocks out of 10% RMS is early in the morning available to the operator before starting the patient examinations. As suggested by the manufacturer, the service is scheduled when the RMS of the block efficiency is > 20% and the scanner use is suspended if a faulty block is reported with zero sensitivity. However, as observed during five years of scanner use, a block damage, detected by daily checks, can be occurred the day before during routine patient examinations without warning to the user. Therefore, knowledge of the malfunctioning block effects in terms of artefacts and diagnostic accuracy loss on reconstructed images can be useful to validate PET studies performed in such scanner conditions.

Aim of the present work is to describe and assess on reconstructed FDG-PET images, different levels of detector failure effects for the HR+, a full ring block designed scanner. For this purpose simulations of different levels of detector defects were performed on test phantoms: a cylinder uniformly filled with a radioactive solution and an anthropomorphic phantom filled with different radioactive solutions representative of ^{18}F-FDG clinical condition. Quantitative evaluations were carried out to identify block detector malfunctioning cases that allow to schedule the maintenance and those that require to stop immediately the clinical activity and call the technical service.

Materials and Methods

Data acquisition

All the measurements were performed on ECAT HR+ (CTI, Knoxville, TN) PET scanner used in 2D mode with extended septa [1]. This block-designed scanner is characterised by four ring of 72 blocks (total 288 blocks) and each block is cut into an 8x8 array of detector elements of 4.39 mm x 4.05 mm x 30 mm size. The gantry has a FOV of 56.2 cm transaxially and 15.5 cm axially covered by 32 detector rings allowing to have in 2D mode 63 transaxial planes (32 direct and 31 crossed). All the 2D acquisitions were done by considering LORs (Line of Responses) of 7 and 8 contiguous axial crystals for direct and crossed planes respectively (Span 15), and 144 angular views (Mash 2X) [1].

Simulation of faulty detectors

The simulation of detector defects was implemented after studying, plane by plane, the specific changes on Blank scan sinograms acquired with the three ^{18}Ge rod sources with and without defective block. For this purpose, retrospectively, were compared couples of contiguous Blank scans one having all detector blocks perfectly working (reference) and one reporting a 100% defective block. The comparison of Blank scans allowed to determine "ad hoc" sinogram maps of multiplicative coefficients (range 0 –1) (Figure 1) to modify efficiency for any of the 288 blocks on original sinograms. Simulations, scripts written in MatLab (The MathWorks, Inc., Natick, MA) for WINDOS 2000, altered original sinograms before any kind of correction.

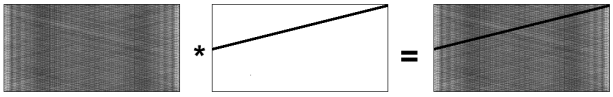

Figure 1. – Left: reference Blank scan; centre:sinogram mask to simulate a block with zero sensitivity; right: altered Blank scan.

ISSN: 1727-1983

Different faulty conditions were simulated:
1) one block detector with a 40% ($B^1_{40\%}$) and 100% ($B^1_{100\%}$) loss of efficiency;
2) one analog board involving 2 contiguous axial blocks, with 40% ($AB_{40\%}$) and 100% ($AB_{100\%}$) loss of efficiency;
3) two opposite blocks in the same plane with 40% and 100% loss of efficiency ($B^1_{40\%}B^2_{100\%}$) and ($B^1_{100\%}B^2_{100\%}$).
For this last case, noting that counting rate (R_{ij}) of two opposite blocks (i,j) is the product of individual efficiencies (εi, εj), with the activity A in the FOV [2]:

$$R_{ij} = \varepsilon_i \cdot \varepsilon_j \cdot A \; ; \qquad (1)$$

the coefficients map was obtained by multiplying the two correspondent maps (Figure 2).

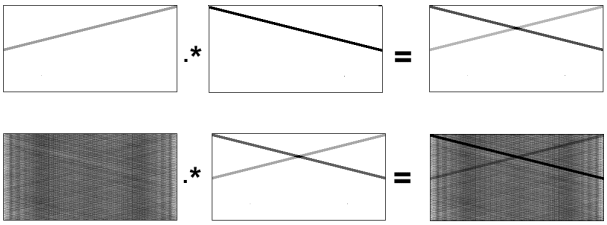

Figure 2. – Simulation of two opposite blocks in the same plane with 40% and 100% loss of efficiency, respectively. Original Blank scan on Bottom-left, altered one on Bottom-right.

Test phantoms

Two different test phantoms were analysed:
- the uniform phantom (20 cm diameter, 24 cm height);
- the anthropomorphic (thorax-abdomen) Alderson phantom (Radiology Support Device Inc., CA) filled with aqueous ^{18}F solutions and containing 4 spherical hot lesions.

Original raw data of these phantoms, acquired with all scanner detectors in good condition, were modified according to the sinogram masks simulating the above described detector defects. The "altered" raw data were then processed using the ECAT standard software for reconstruction.

The uniform phantom was acquired following the NEMA NU 2-1994 [3] and reconstructed with standard FBP with 0.5 cut-off ramp and also with OSEM algorithm by setting different iterations and subsets (2i/8s, 4i/16s and 4i/32s) to take into consideration also the reconstruction algorithm dependence. For this particular test phantom, being uniform, a single angular defective view was considered as shown on Figure 3.

For the Alderson phantom, the different anatomical districts were filled with different aqueous radioactive solutions to represent the in vivo ^{18}F-FDG uptake. To fully describe clinical conditions, whole-body acquisition procedures used for patient studies were as well considered. The phantom scan was covered by 3 beds of 6 min acquisition each, 4 min emission and 2 min post injection transmission in sequence (ETTE). All the raw data were reconstructed with OSEM (2i/8s) as routinely used in whole-body PET FDG studies and (4i/16s) to improve image contrast.

Data analysis

All reconstructed images were visually inspected by expert observers.

For the reconstructed images of the uniform phantom the standard coefficient of variation (CV%), was assessed on original and modified data. Regional decrease of counts in terms of percent difference ($\Delta_{\%}C_{mean}$) was also determined by comparing mean counts of the 9 ROIs (see Figure 3 Right) drawn on the original and altered images.

For the anthropomorphic phantom 4 different ROIs were positioned on different districts (liver, mediastinum, heart and hot lesions) of original and altered images. The percent difference $\Delta SUV_{\%}$ of SUV (standarized uptake value) was assessed by comparing ROIs of the two data set.

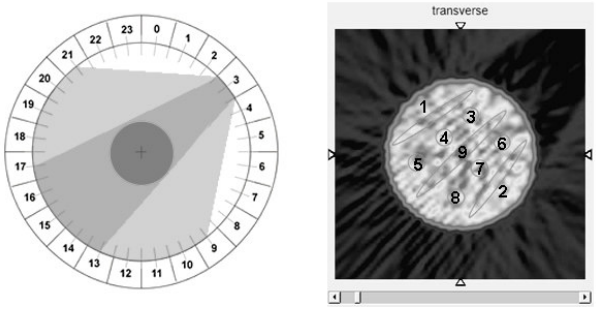

Figure 3 – Left: Typical angular view (Fan angle) of one block detector; Right: Tomographic section of the uniform phantom including the 9 ROIs used for quantitative analysis.

Results

Visual inspection of the uniform phantom, according to observations reported by other authors [4], confirmed that reconstructed images of planes including defective block having even 100% efficiency loss, in spite of evident defect on sinograms (cold diagonal bands), are affected by slight artefacts. These appears as cold stripes following the Fan angle covered by the defective detector (Figure 3 -Right). This phantom, by irradiating uniformly all the detectors, allowed to measure on reconstructed image the degradation of uniformity due to the loss of sensitivity corresponding to cold stripes. By comparing quantitative data obtained on original and altered phantoms, (see Tables 1.a) and b)), it is evident that 1 block with 100% loss of efficiency slightly increases CV%, a non-uniformity parameters not significatively different from the value measured on original data. More important variations are observed when two opposite blocks in the same plane, both with 100% inefficiency, are considered (Figure 4). In this case, depending on the geometrical position of the two blocks, a well structured artefact along the direct coincidence line is visible and a peak-valley count distribution affects the image. This case is

ISSN: 1727-1983

better documented by the line profile of Figure 5.c: the main peak, apparent increase of counts, corresponds to the hyperactive stripe. The quantitative evaluation in terms of $\Delta_{\%}C_{mean}$, reported in Table 2, demonstrated that the amount of regional count changes increases by using reconstruction parameters allowing increased image contrast .

Table 1.a) Uniform phantom: non-uniformity measures.

Index	Original	$B^1_{100\%}$	$AB_{100\%}$	$B^1_{100\%}$ $B^2_{100\%}$
$CV_{\%}$	3.5 ±0.5	3.9	4.4	5

Table 1.b) Uniform phantom: non-uniformity measures.

Index	Original	$B^1_{40\%}$	$AB_{40\%}$	$B^1_{40\%}$ $B^2_{100\%}$
$CV_{\%}$	3.5 ±0.5	3.5	3.7	3.9

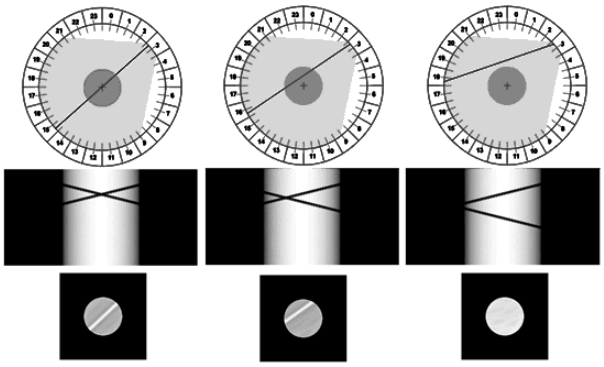

Figure 4. Uniform phantom acquired with two opposite blocks with 100% and 40% loss of efficiency, respectively. From top to bottom: blocks geometrical positions; correspondent phantom sinograms; reconstructed phantom images.

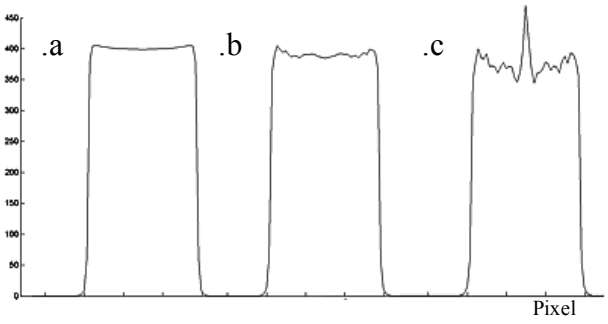

Figure 5. Line profiles crossing the section of the original (a), the section simulating $B^1_{100\%}$ (b) and the section simulating the two opposite blocks $B^1_{100\%}$ $B^2_{100\%}$ (c) of the uniform phantom.

Table 2. Uniform phantom: $\Delta_{\%}C_{mean}$,.values.

Algorithm	$B^1_{100\%}$	$B^1_{40\%}$	$AB_{100\%}$	$AB_{40\%}$	$B^1_{100\%}$ $B^2_{100\%}$	$B^1_{40\%}$ $B^2_{100\%}$
FBP	5	2	7	2	8	6
2i/8s	5	3	5	3	9	5
4i/16s	7	4	6	4	10	7
4i/32s	17	8	12	8	17	14

Evaluation of detection inefficiency on reconstructed images of the anthropomorphic Alderson phantom are presented below. As shown on Figure 6.a no artefacts visually appear on reconstructed images using clinical protocols (2i/8s and 4i/16s OSEM) but, when image differences (original-altered images) are generated Fan angle count distribution is still evident (Figure 6.b). On altered images, reduction of block sensitivity induces a systematic decrease of SUV values, along the hypoactive stripe artefacts. A maximum $\Delta SUV_{\%}$ value of -3% corresponds to 100% block detector inefficiency (see Table 3). A -4% $\Delta SUV_{\%}$ value was measured for $AB_{100\%}$.

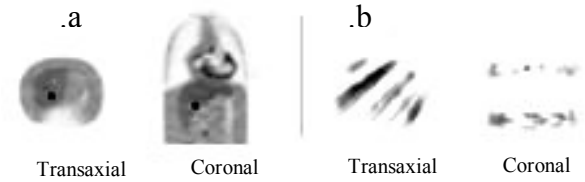

Figure 6. a) Reconstructed images (OSEM 2i/8s) of the Alderson phantom; b) image differences scaled to the maximum value.

The worst condition, as shown on Table 4, corresponds to two opposite defective blocks with 100% loss efficiency when maximum $|\Delta SUV_{\%}|$ values of 5.4% and 15.1% are respectively measured with 2i/8s and 4i/16s OSEM. It is worth considering that this particular case from a clinical point of view is less under control as the SUV can increase or decrease depending on the hyper or hypo-active stripe artefacts position.

Table 3. Maximum percent differences of SUV values measured when 1 block is simulate with 40% and 100% loss of efficiency.

Max $\Delta SUV_{\%}$	$B^1_{40\%}$		$B^1_{100\%}$	
	2i/8s	4i/16s	2i/8s	4i/16s
ROI_1	-0.2	-0.2	-1.2	-2.0
ROI_2	-0.1	0.1	-2.9	-3.2
ROI_3	-0.8	-0.8	-1.0	-1.0
ROI_4	-0.8	-0.6	-1.3	-1.8

ISSN: 1727-1983

Table 4. Percent differences of maximum SUV values measured when two opposite defective blocks are in the same plane

Max $\Delta SUV_{\%}$	$B^1_{40\%}$ $B^2_{100\%}$		$B^1_{100\%}$ $B^2_{100\%}$	
	2i/8s	4i/16s	2i/8s	4i/16s
ROI_1	|-0.3|	|-1.4|	|-0.7|	|-5.3|
ROI_2	|3.1|	|4.3|	|5.4|	|15.1|
ROI_3	|-1.5|	|-7.5|	|-4.5|	|-4.5|
ROI_4	|1.3|	|4.4|	|2.1|	|3.4|

Discussion and conclusion

The present work aimed to study potential artefacts on reconstructed images caused by detector damages. Different levels of block-detectors efficiency loss were simulated to alter original image of test phantoms acquired with the ECAT HR+ PET scanner operating in good detection conditions. Two phantoms were considered, one having a uniform radioactive distribution acquired at high counting statistics and one simulating ^{18}F-FGD patient uptake following clinical procedures. For both the phantoms visual and quantitative analysis were carried out, to estimate how some faulty detector can alter reconstructed images. As expected, all reconstructed altered images are characterised by an overall decrease of counts as consequence of the simulated loss of detector efficiency. However this reduction is not uniformly distributed but Fan shaped depending on the particular geometrical position of the defective block. Images of this uniform source, obtained at high counting statistics, demonstrated that non-uniformity parameters did not significatively change whenever assessed on original or on altered data having 1 block or 2 axial blocks (faulty analog board) with zero sensitivity. Different is the case when 100% loss of efficiency involves two opposite blocks in the same plane; this represented the worst condition either visually (well evident hyperactive stripe) and quantitatively (significant changes of CV%) .

The analysis on the anthropomorphic phantom allowed to establish how the considered degrees of faulty detection can change clinical meanings or the assessment of lesion SUV. When 1 block/plane is defective for even 100% loss of efficiency, a maximum of 3-4% decrease in SUV can be measured. The entity of this variation, can be considered not clinically relevant either for staging or for following-up oncological lesions. Without intending to lower scanner quality standards but to avoid practical problems in patient routine management, when such faulty conditions occur, call of maintenance service is scheduled as soon as possible but in the meanwhile planned clinical studies can be performed. Different is the case of 2 opposite blocks/plane with 100% loss of efficiency. In this scanner status, using 4i/16s OSEM, increase or decrease of SUV larger than $\pm$15%, can be found on particular body regions coincident with structured artefact positions. Therefore it is important to well identify each of the analysed defects with the help of the daily Blank scan. When 100% loss of efficiency for two opposite defective blocks exists it is strongly recommended to stop clinical activity and scanner maintenance is required.

It is worth noting that all the considerations addressed to the possibility to use the scanner also with defective block must be interpreted as an help in clinical routine and not to lower quality assurance or reduce frequency maintenance.

All the presented simulations regarding defective blocks with loss of efficiency are specific for ECAT HR+ scanner; cases with increased efficiency is also useful and are under investigation. Results of quantitative analysis obtained in the present work cannot be extended directly to other type of full-ring PET scanners which require individual evaluations.

In conclusion, this study showed that for HR+ scanner, a fault (100% loss of efficiency) of a single block or an analog board (2 axial blocks) particular evident on sinograms does not substantially affect qualitatively and quantitatively FDG whole-body reconstructed images (SUV % variations less than 4%). When two opposite blocks in the same plane have 100% loss of efficiency larger inaccuracy should be expected and in this case stopping clinical activity is claimed. However, all defective block considerations referred as to be not relevant for scanner clinical use must be utilised to avoid practical problems in temporary patient management and not to change maintenance scheduler or lower the quality standards.

References

[1] BRIX G, ZAERS J et al. ,(1997). 'Performance Evaluation of a Whole-Body PET Scanner Using the NEMA Protocol', *J Nucl Med*; **38**, pp. 1614-1623

[2] CASEY ME., HOFFMAN EJ., (1986): 'Quantitation in Positron Emission Computed Tomography: a technique to reduce noise in accidental coincidence measurements and coincidence efficiency calibration', J. *Comput. Assist. Tomogr.*, **10**, pp. 845-850

[3] NEMA STANDARDS PUBL. NU 2-1994 (1994): 'Performance Measurements of Positron Emission Tomographs', *Nat. Elect.Manufacturers Assoc*.

[4] TOWNSEND DW. (1996): 'Quality control of PET scanner', 8th Annual International PET Conference.

[5] BUCHERT R., BOHUSLAVIZKI KH., MESTER J., CLAUSEN M. (1999): 'Quality assurance in PET: evaluation of the clinical relevance of detector defects', *J Nucl Med*; **40**, pp. 1657-1665

[6] THIE JA., HUBNER KF., SMITH GT. (2000): 'The Diagnostic Utility of the Lognormal Behavior of PET Standardized Uptake Values in Tumors', *J Nucl Med*; **41**, pp. 1664-1672

ISSN: 1727-1983